

A Point-Source Catalog from *Swift* Observations of Unidentified *Fermi* Sources

N. Mirabal^{1,2}

Received _____; accepted _____

¹Ramón y Cajal Fellow; Dpto. de Física Atómica, Molecular y Nuclear, Universidad Complutense de Madrid, Spain

²Email: mirabal@gae.ucm.es

ABSTRACT

We present X-ray point source catalogs obtained from archival *Swift* observations that have partially or fully covered the 95% confidence error contour of unidentified *Fermi* sources. In total, 21 out of 37 unidentified *Fermi* sources have been observed by the X-Ray Telescope (XRT) on board the *Swift* observatory. Basic properties such as position, positional errors, count rates, and hardness ratios are derived for a total of 18 X-ray point sources found in the sample. From these detections, we discuss potential counterparts to 0FGL J0910.2–5044, 0FGL J1045.6–5937, 0FGL J1115.8–6108, 0FGL J1231.5–1410, 0FGL J1326.6–5302, 0FGL J1604.0–4904, and 0FGL J1805.3–2138. The catalog will assist observers planning future programs to identify 0FGL sources without obvious counterparts.

Subject headings: gamma rays: observations – X-rays: general

1. Introduction

Until recently, nearly the totality of γ -ray sources in the inner Galaxy $l = 270^\circ - 90^\circ$ and $-30^\circ < b < 30^\circ$ remained without firm counterparts. It has been long suspected that low-latitude sources comprise a Galactic population that is either similar to the already identified γ -ray pulsars (Yadigaroglu & Romani 1997), or represent an entirely new class of γ -ray emitters associated with the disk/bulge population (Thompson 2008; Johnson & Mukherjee 2009). With improved localizations and superb timing capabilities, *Fermi* has started to unveil the likely culprits (Abdo et al. 2009b). Among the sources reported in the Bright Gamma-ray Source List (0FGL), 26 include pulsars, supernova remnants, and pulsar wind nebulae (Roberts 2005) within the inner Galaxy. While we are certainly on our way to solving this long-standing puzzle, the nature of approximately half of the 0FGL sources in the inner Galaxy remains elusive.

It is likely that additional *Fermi* sources will be identified through γ -ray timing. Others will require intensive work at other wavelengths to produce plausible counterparts. Important challenges await for sources that fail to reveal themselves easily. Radio surveys will be of limited help for the potential analogs to the radio-quiet pulsars such as 0FGL J0007.4+7303 (Halpern et al. 2004; Abdo et al. 2009a) and 0FGL J1836.2+5925 (Mirabal & Halpern 2001; Reimer et al. 2001; Halpern et al. 2002; Abdo et al. 2009c). In addition, extreme dust extinction and reddening close to the Galactic plane will be difficult to overcome in the optical. As a consequence, hard X-rays may provide the only opportunity to penetrate the Galactic barrier and gain access to γ -ray objects in the inner Galaxy.

X-ray observations were crucial in recent efforts to secure likely counterparts for a pair of unidentified *Fermi* sources (Bassani et al. 2009; Mirabal & Halpern 2009). In order to extend the X-ray efforts and to help foster multiwavelength collaborations, we present X-ray

point source catalogs derived from archival *Swift* observations of unidentified *Fermi* sources. The paper is organized as follows. Section 2 describes the observations and data reductions. Sections 3 and 4 provide details about individual *Fermi* sources. Lastly, discussion and conclusions are presented in Section 5.

2. Observations and Data Reduction

Data for unidentified *Fermi* sources were retrieved from the public *Swift* archive and comprise observations obtained during 3 November 2005–5 August 2009. In this period, a total of 21 unidentified *Fermi* sources were partially or fully covered with the X-Ray Telescope (XRT) on board *Swift* (Gehrels et al. 2004). Figure 1 shows the distribution of unidentified *Fermi* sources gathered from Abdo et al. (2009b) and highlights the *Fermi* contours covered by *Swift* observations. All observations were obtained with the XRT operated in photon counting (PC) mode. The details of *Swift* XRT observations of unidentified *Fermi* sources are summarized in Table 1.

Source extraction to identify all significant X-ray sources within the *Fermi* error contours was performed with *wavdetect*. Source positions and positional errors were derived using *xrtcentroid*. X-ray counts (0.3–10 keV) were extracted from a circular region with a 20 pixel radius (47"). The background was extracted from an annulus with a 20 pixel (inner radius) to 30 pixel (outer radius) around the source. Throughout, we used *XSELECT* to filter counts with grades 0–12. In fields without significant detections, we placed upper limits to the presence of point source emission for the particular *Swift* observation. X-ray point sources detected within the 95% confidence error contour of unidentified *Fermi* sources are listed in Tables 2–16. Figures that show the 95% *Fermi* error contours superimposed

on smoothed *Swift* XRT images can be found at our website¹.

In addition to position and count rate, we also computed the hardness ratio (HR) after separating the 2–10 keV *hard* band (H) count rate and the 0.3–2 keV *soft* band (S) count rate for each source. The ratio itself was derived by adopting $HR = \frac{H-S}{H+S}$. As a result, negative values of HR indicate softer X-ray sources. We caution that certain unidentified *Fermi* sources suffer from large Galactic H I column densities N_{H} (fifth column of Tables 2–16) as derived from the nH tool². In such cases, the observed HR most likely underestimates the actual amount of photons in the *soft* 0.3–2 keV band.

3. Notes on Individual Objects

0FGL J0614.3–3330: This source is listed as 3EG J0616–3310 in the 3EG catalog (Hartman et al. 1999). Within the the *Fermi* 95% confidence error contour lies the relatively soft X-ray source Swift J0614.5–3332. An *XMM-Newton* object consistent with this position was suggested by La Palombara et al. (2007) as the counterpart of 3EG J0616–3310. There are no archival radio sources consistent with the X-ray position.

0FGL J0910.2–5044: Abdo et al. (2009b) declare this source variable in γ -rays. The X-ray source Swift J0910.9–5048 is likely associated with a blazar (Sadler 2008) and Galactic plane transient at $b = -1.^\circ 8$ (Cheung et al. 2008; Landi et al. 2008).

0FGL J1231.5–1410: Detected as EGR J1231–1412 in the EGR catalog (Casandjian & Grenier 2008). The brightest source in the field, Swift J1231.1–1411, lacks a radio counterpart in the NRAO VLA Sky Survey (NVSS) source catalog (Condon et al.

¹See <http://www.gae.ucm.es/~mirabal/Unidentified.html>

²<http://heasarc.gsfc.nasa.gov/cgi-bin/Tools/w3nh/w3nh.pl>

1998). The source is soft in X-rays with a hardness ratio $HR = -1.00$, *i.e.* all its X-ray photons are detected at energies $E < 2.0$ keV. Inspection of a Digitized Sky Survey image reveals a blank field at the X-ray position down to a conservative limit of $R > 20.1$. We argue that Swift J1231.1–1411 meets the requirements of a potential neutron-star counterpart to 0FGL J1231.5–1410.

0FGL J1311.9–3419: Listed as 3EG J1314–3431 in the third EGRET catalog. Sowards-Emmerd et al. (2004) proposed the radio source J1316–3338 as the likely counterpart for the original EGRET error contour. However, this association is now excluded by the Fermi localization. The sole X-ray source in this region, Swift J1311.5–3418, could be associated with NVSS J131130.97–341810.5 detected with a flux density 13.8 mJy at 1.4 GHz.

0FGL J1326.6–5302: We find a single X-ray source, Swift J1326.8–5256, within the *Fermi* error contour. A corresponding radio source PMN J1326–5256 was proposed by Mirabal & Halpern (2009) as the likely counterpart of 0FGL J1326.6–5302. PMN J1326–5256 was also tentatively associated with unidentified EGRET source 3EG J1316–5244 (Bignall et al. 2008).

0FGL J1413.1–6203: Originally discovered by COS B (catalog name 2CG 311–01) and later confirmed by EGRET (3EG) and AGILE 1AGL J1412–6149 (Pittori et al. 2009). No X-ray sources brighter than 2.5×10^{-3} s⁻¹ are detected within the *Fermi* error contour. PSR J1412–6145 and J1413–6141 were proposed as possible counterparts of the original EGRET source (Torres, Butt & Camilo 2001). However, both of these pulsars appear to be excluded as counterparts with the new LAT position. The LAT contour still embeds faint shell arcs possibly associated with the supernova remnant G312.4–0.4 (Case & Bhattacharya 1999; Doherty et al. 2003). However, the main shell structure of the remnant lies outside the Fermi error contour.

0FGL J1536.7–4947: Swift J1536.2–4944 is the only prominent X-ray source in the *Fermi* 95% confidence error contour. The source is positionally consistent with an extended radio source MRC 1532–495A clearly visible at 843 MHz (Jones & McAdam 1992). A corresponding radio source PMNM 153234.4–493426 was also detected in the Green Bank 4.85 GHz northern sky survey carried out during 1986 November and 1987 October (Gregory et al. 1996).

0FGL J1604.0–4904: Inside the *Fermi* error contour lies a single source Swift J1603.8–4904. The X-ray source is also detected in radio as PMN J1603–4904 at 4.85 GHz with a flux density of 954 mJy. It appears to be an excellent blazar candidate.

0FGL J1634.9–4737: No X-ray sources were detected in the *Swift* pointing down to $2.7 \times 10^{-3} \text{ s}^{-1}$. We note that the Soft Gamma Ray Repeater SGR 1627–41 is localized outside the *Fermi* error contour.

0FGL J1653.4–0200: Previously detected as 3EG J1652–0223 by EGRET (Hartman et al. 1999). A radio pulsar search of the original EGRET error circle with the Parkes 64–m radio telescope failed to detect a plausible counterpart (Crawford et al. 2006). Two X-ray sources Swift J1653.3–0158 and Swift J1653.9–0203 are detected within the *Fermi* error circle.

0FGL J1805.3–2138: Lies in the vicinity of the TeV source HESS J1804–216 (Kargaltsev et al. 2007). This field was partially covered by Swift. One intriguing X-ray source Swift J1804.5–2140 is detected within the *Fermi* error contour. Kargaltsev et al. (2007) suggested that the latter could be an accreting binary or a pulsar wind nebula possibly associated with HESS J1804–216. However, no convincing evidence for pulsations has been found.

0FGL J1813.5–1248: Initially listed as unidentified in the original 0FGL release.

The γ -ray pulsar PSR 1813–1246 was later revealed at this position (Abdo et al. 2009b). Swift J1813.4–1246 most likely corresponds to the X-ray counterpart to this source. One puzzle regarding this source concerns the fact that 0FGL J1813.5–1248 is the only *Fermi* pulsar listed as variable in the 0FGL. If real, the γ -ray variability could be indicative of a multiple sources overlapping in the same line of sight (i.e. a γ -ray pulsar and γ -ray blazar in the same region of the sky). Alternatively 0FGL J1813.5–1248 may well be a very peculiar γ -ray pulsar.

0FGL J1830.3+0617: We find a single X-ray source, Swift J1830.1+0619, within the *Fermi* error contour. Mirabal & Halpern (2009) have identified this blazar as the likely counterpart of 0FGL J1830.3+0617.

0FGL J2001.0+4352: Two sources lie within the the *Fermi* error contour. Of these, Swift J2001.2+4352 was proposed by Bassani et al. (2009) as the counterpart of 0FGL J2001.0+4352.

0FGL J2027.5+3334: No prominent X-ray sources brighter than $1.5 \times 10^{-3} \text{ s}^{-1}$ are detected within the *Fermi* 95% confidence error contour.

0FGL J2055.5+2540: Two X-ray sources lie within the *Fermi* error circle. Neither Swift J2055.8+2546 nor Swift J2055.8+2540 have apparent counterparts at 1.4 GHz.

0FGL J2241.7–5239: Not detected by EGRET or AGILE. One significant source Swift J2241.5–5246 lies at the edge of the *Fermi* 95% confidence error contour. This X-ray source appears to have a radio equivalent in the stamp image extracted from the 843 MHz Sydney University Molonglo Sky Survey (Bock et al. 1999).

0FGL J2302.9+4443: One low significant X-ray source was detected at edge of *Fermi* error contour on 2009 February, 15. Intriguingly, Swift J2302.1+4445 was not detected in a second *Swift* pointing conducted ≈ 16 days later. The reality of this source

requires further confirmation.

4. Special Cases

A keen reader will notice the omission of three additional unidentified *Fermi* sources that have been covered by *Swift* namely 0FGL J1045.6–5937, 0FGL J1115.8–6108, and 0FGL J1746.0–2900. We have deliberately labeled these sources as special cases given the complexity of said regions.

0FGL J1045.6–5937: First observed as γ -ray source 1AGL J1043–5931 by the AGILE satellite (Tavani et al. 2009). The *Fermi* 95% confidence error contour contains the colliding wind binary Eta Carinae and the Carina nebula (NGC 3372). This region has been observed by *Swift* and other major X-ray missions in multiple occasions. The γ -ray emission could be produced due to the interaction of colliding winds associated with the Eta Carinae binary system (Benaglia et al. 2005; Reimer & Reimer 2009). However, an alternative γ -ray emitter cannot be excluded. One interesting candidate is the neutron star candidate XMM J104608.72–594306.5 discovered by Hamaguchi et al. (2009).

0FGL J1115.8–6108: This field contains the starburst region NGC 3603 located in the Carina spiral arm. It has been observed by *Swift* in three separate visits. The massive stellar population in this region includes numerous OB and Wolf-Rayet stars. The reader is referred to Moffat et al. (2001) for a detailed analysis. Among the massive star population, the binary system WR43a stands out. Moffat et al. (2001) argued that the scatter observed in some of the most luminous X-ray sources in NGC 3603 may indicate the presence of additional colliding wind binaries. As a result, it is important to investigate whether massive colliding wind binaries are driving the γ -ray production associated with this source. Nevertheless, alternative emitters cannot be ruled out with the current observations.

0FGL J1746.0–2900: Possibly associated with the Galactic Center region. This general area has been observed multiple times by *Swift*. Unfortunately, cataloguing and modeling the X-ray emission is challenging. We refer the reader to Munro et al. (2005) for a point-source catalog of this region.

5. Discussion and Conclusions

We have presented point-source catalogs and data analyses of 24 *Swift* XRT individual observations that have partially or fully covered the error contours of unidentified *Fermi* sources. In total, we have detected 18 X-ray point sources distributed over 15 unidentified *Fermi* error contours. For 0FGL J1413.1–6203, 0FGL J1634.9–4737, and 0FGL J2027.5+3334 we are only able to derive upper limit for source detections. In addition to positions and count rates, we have computed the hardness ratios of detected sources.

With a uniform dataset at hand, it is critical to examine these X-ray point sources as potential counterparts to unidentified *Fermi* sources. We have advanced initial interpretations for a handful. However, additional efforts are required to further characterize the nature of the remaining counterpart candidates. It is our hope that this catalog release will motivate multiwavelength collaborations and help plan future observational programs. In particular, as shown here continued observations with *Swift* and other major X-ray observatories will be key in advancing the identification of *Fermi* sources within the inner Galaxy. In order to ensure quick access to newer versions of this catalog, we will provide regular updates through our website ³.

I thank the Spanish Ministry of Science and Technology for support through a Ramón

³See <http://www.gae.ucm.es/~mirabal/Unidentified.html>

y Cajal fellowship. I acknowledge illuminating correspondence with Jules Halpern and Michael T. Wolff. I also gratefully acknowledge Teddy Cheung, David Thompson, and the rest of the *Fermi* team for promoting the early multiwavelength efforts.

REFERENCES

- Abdo, A. A., et al. 2009a, *Science*, 322, 1218
- Abdo, A. A., et al. 2009b, *ApJS*, 183, 46
- Abdo, A. A., et al. 2009c, *Scienceexpress*, 10.1126
- Bassani, L., Landi, R., Masetti, N., Parisi, P., Bazzano, A., & Ubertini P. 2009, *MNRAS*, 397, L55
- Benaglia, P., Romero, G. E., Koribalski, B., & Pollock, A. M. T., 2005, *A&A*, 440, 743
- Bignall, H., Cimo, G., Jauncey, D., Senkbeil, C., Lovell, J., & Ellingsen, S. 2008, arXiv:0805.3891
- Bock, D. C.-J., Large, M. I., & Sadler, E. M. 1999, *AJ*, 117, 1578
- Casandjian, J.-M. & Grenier, I. A. 2008, *A&A*, 489, 849
- Case, G. & Bhattacharya, D. 1999, *ApJ*, 521, 246
- Cheung, C. C., Reyes, L., Longo, F., & Iafrate, G., ATel 1788
- Condon, J. J., Cotton, W. D., Greisen, E. W., Yin, Q. F., Perley, R. A., Taylor, G. B., & Broderick, J. J. 1998, *AJ*, 115, 1693
- Crawford, F., et al. 2006, *ApJ*, 652, 1499
- Doherty, M., Johnston, S., Green, A. J., Roberts, M. S. E., Romani, R. W., Gaensler, B. M., & Crawford, F. 2003, *MNRAS*, 339, 1048
- Gehrels, N., et al. 2004, *ApJ*, 1005
- Gregory, P. C., Scott, W. K., Douglas, K., & Condon J. J. 1996, *ApJS*, 103, 427

- Halpern, J. P., Gotthelf, E. V., Mirabal, N., & Camilo, F. 2002, *ApJ*, 573, L41
- Halpern, J. P., Gotthelf, E. V., Camilo, F., Helfand, D. J., & Ransom, S. M. 2004, *ApJ*, 612, 398
- Hamaguchi, K., et al. 2009, *ApJ*, 695, L4
- Hartman, R. C., et al. 1999, *ApJS*, 123, 79
- Johnson, R. P., & Mukherjee, R. 2009, *New J. Phys.*, 11, 055008
- Jones, P. A., & McAdam, W. B. 1992, *ApJS*, 80, 137
- Kargaltsev, O., Pavlov, G. G., & Garmire, G. P. 2007, *ApJ*, 670, 643
- Landi, R., Sguera, V., Bassani, L., Bazzano, A., De Rosa, A., & Dean, A. J. 2008, *ATel* 1822
- La Palombara, N., Mignani, R. P., Hatziminaoglou, E., Schirmer, M., Bignami, G. F., & Caraveo, P. 2007, *Ap&SS*, 309, 209
- Mirabal, N., & Halpern, J. P. 2001, *ApJ*, 547, L137
- Mirabal, N., & Halpern, J. P. 2009, *ApJ*, 701, L129
- Moffat, A. F. J., et al. 2001, *ApJ*, 573, 191
- Muno, M. P., Pfahl, E., Baganoff, F. K., Brandt, W. N., Ghez, A., Lu, J., & Morris, M. R. 2005, *ApJ*, 622, L113
- Pittori, C. et al. 2009, *A&A*, in press
- Reimer, O., Brazier, K. T. S., Carramiñana, A., Kanbach, G., Nolan, P. L., & Thompson, D. J. 2001, *MNRAS*, 324, 772

Reimer, A., & Reimer, O. 2009, *ApJ*, 694, 1139

Roberts, M. S. E. 2005, *Adv. Space Res.*, 35, 1142

Sadler, E. 2008, ATel 1843

Sowards-Emmerd, D., Romani, R. W., Michelson, P. F., & Ulvestad, J. S. 2004, *ApJ*, 609,
564

Tavani, M., et al. 2009, *ApJ*, 698, L42

Thompson, D. J. 2008, *Rep. Prog. Phys.*, 71, 116901

Torres, D. F., Butt, Y.M., & Camilo, F. 2001, *ApJ*, 560, L155

Yadigaroglu, I. A., & Romani, R. W. 1997, *ApJ*, 476, 347

Table 1. Unidentified *Fermi* sources observed by *Swift*

Name OFGL	ObsID	Date	Start Time UT	Exposure (sec)
J0614.3–3330	00031375001	2009-03-16	06:45:35	3550
J0910.2–5044	00031282001	2008-10-17	02:18:51	7188
	00031282002	2008-10-18	02:25:20	4686
	00031282003	2008-11-17	15:13:22	5295
J1045.6–5937	00090033001	2009-03-24	08:44:01	14363
J1115.8–6108	00090051001	2008-04-23	04:50:01	3048
J1231.5–1410	00031354001	2009-02-24	18:07:41	4175
J1311.9–3419	00031358001	2009-02-27	18:24:02	3352
J1326.6–5302	00031458001	2009-08-05	14:37:45	4866
J1413.1–6203	00031410002	2009-05-13	00:35:18	3232
J1536.7–4947	00090193001	2009-06-20	02:30:01	1008
J1604.0–4904	00039227001	2009-05-13	05:03:03	772
J1634.9–4737	00312579016	2008-07-31	06:44:26	5285
J1653.4–0200	00031379001	2009-03-22	00:28:57	4786
J1746.0–2900	00035063094	2006-06-15	00:49:01	17528
J1805.3–2138	00035156001	2005-11-03	01:15:42	11508
J1813.5–1248	00031381001	2009-03-26	18:27:26	3232
	00031381002	2009-03-27	00:53:14	2314
	00031381003	2009-03-29	04:22:02	3974
	00090197001	2009-06-12	09:30:36	2259
J1830.3+0617	00039228001	2009-05-20	04:41:20	580
J2001.0+4352	00039229001	2009-06-12	07:00:38	7334
J2027.5+3334	00090200001	2009-04-26	18:30:24	3490
J2055.5+2540	00031391001	2009-04-02	16:13:06	4749
J2241.7–5239	00031384001	2009-03-26	00:50:34	3851
J2302.9+4443	00031346001	2009-02-15	02:07:03	5175
	00031346002	2009-03-01	17:52:37	3934

Table 2. 0FGL J0614.3–3330

Source	RA (J2000)	Decl. (J2000)	Positional error	Count rate (0.3–10 keV)	HR $\frac{H-S}{H+S}$	N_{H} (cm^{-2})	ObsID
Swift J0614.5–3332	06:14:30.0	-33:32:22	6."5	$(4.5 \pm 1.1) \times 10^{-3} \text{ s}^{-1}$	-0.73	3.5×10^{20}	00031375001

Table 3. 0FGL J0910.2–5044

Source	RA (J2000)	Decl. (J2000)	Positional Error	Count rate (0.3–10 keV)	HR $\frac{H-S}{H+S}$	N_{H} (cm^{-2})	ObsID
Swift J0910.9–5048	09:10:57.4	-50:48:11	4."6	$(6.0 \pm 1.1) \times 10^{-3} \text{ s}^{-1}$	0.49	1.0×10^{22}	00031282001
	09:10:57.5	-50:48:09	4."8	$(1.0 \pm 0.1) \times 10^{-2} \text{ s}^{-1}$	0.72	1.0×10^{22}	00031282002
	09:10:57.7	-50:48:05	4."8	$(7.4 \pm 1.2) \times 10^{-3} \text{ s}^{-1}$	0.88	1.0×10^{22}	00031282003

Table 4. 0FGL J1231.5–1410

Source	RA (J2000)	Decl. (J2000)	Positional error	Count rate (0.3–10 keV)	HR $\frac{H-S}{H+S}$	N_{H} (cm^{-2})	ObsID
Swift J1231.1–1411	12:31:11.3	-14:11:43	5."6	$(5.5 \pm 1.2) \times 10^{-3} \text{ s}^{-1}$	-1.00	3.4×10^{20}	00031354001

Table 5. 0FGL J1311.9–3419

Source	RA (J2000)	Decl. (J2000)	Positional error	Count rate (0.3–10 keV)	HR $\frac{H-S}{H+S}$	N_{H} (cm^{-2})	ObsID
Swift J1311.5–3418	13:11:30.5	-34:18:11	6."0	$(6.4 \pm 1.4) \times 10^{-3} \text{ s}^{-1}$	-0.76	5.0×10^{20}	00031358001

Table 6. 0FGL J1326.6–5302

Source	RA (J2000)	Decl. (J2000)	Positional error	Count rate (0.3–10 keV)	HR $\frac{H-S}{H+S}$	N_{H} (cm^{-2})	ObsID
Swift J1326.8–5256	13:26:49.4	-52:56:26	3.''9	$(4.2 \pm 0.3) \times 10^{-2} \text{ s}^{-1}$	-0.03	1.9×10^{21}	00031458001

Table 7. 0FGL J1536.7–4947

Source	RA (J2000)	Decl. (J2000)	Positional error	Count rate (0.3–10 keV)	HR $\frac{H-S}{H+S}$	N_{H} (cm^{-2})	ObsID
Swift J1536.2–4944	15:36:11.7	-49:44:57	7.''3	$(1.3 \pm 0.4) \times 10^{-2} \text{ s}^{-1}$	0.14	3.5×10^{21}	00090193001

Table 8. 0FGL J1604.0–4904

Source	RA (J2000)	Decl. (J2000)	Positional error	Count rate (0.3–10 keV)	HR $\frac{H-S}{H+S}$	N_{H} (cm^{-2})	ObsID
Swift J1603.8–4904	16:03:50.5	-49:04:02	8.''6	$(1.0 \pm 0.4) \times 10^{-2} \text{ s}^{-1}$	-0.25	7.9×10^{21}	00039227001

Table 9. 0FGL J1653.4–0200

Source	RA (J2000)	Decl. (J2000)	Positional error	Count rate (0.3–10 keV)	HR $\frac{H-S}{H+S}$	N_{H} (cm^{-2})	ObsID
Swift J1653.3–0158	16:53:15.4	-01:58:22	4.''1	$(2.5 \pm 0.4) \times 10^{-2} \text{ s}^{-1}$	-0.53	8.3×10^{20}	00031379001
Swift J1653.9–0203	16:53:58.7	-02:03:15	5.''1	$(5.8 \pm 1.1) \times 10^{-3} \text{ s}^{-1}$	-0.31	8.3×10^{20}	00031379001

Table 10. 0FGL J1805.3–2138 (Partially covered)

Source	RA (J2000)	Decl. (J2000)	Positional error	Count rate (0.3–10 keV)	HR $\frac{H-S}{H+S}$	N_{H} (cm^{-2})	ObsID
Swift J1804.5–2140	18:04:32.3	-21:40:10	4.''6	$(1.8 \pm 0.5) \times 10^{-3} \text{ s}^{-1}$	1.00	1.1×10^{22}	00035156001

Table 11. 0FGL J1813.5–1248

Source	RA (J2000)	Decl. (J2000)	Positional error	Count rate (0.3–10 keV)	HR $\frac{H-S}{H+S}$	N_{H} (cm^{-2})	ObsID
Swift J1813.4–1246	18:13:23.5	-12:46:00	5."0	$(8.1 \pm 1.8) \times 10^{-3} \text{ s}^{-1}$	0.96	6.6×10^{21}	00031381001
	18:13:23.5	-12:46:03	7."1	$(5.2 \pm 1.6) \times 10^{-3} \text{ s}^{-1}$	0.50	6.6×10^{21}	00031381002
	18:13:23.3	-12:46:01	4."8	$(7.2 \pm 1.5) \times 10^{-3} \text{ s}^{-1}$	1.00	6.6×10^{21}	00031381003
	18:13:23.6	-12:46:04	6."0	$(7.5 \pm 1.5) \times 10^{-3} \text{ s}^{-1}$	0.50	6.6×10^{21}	00090197001

Table 12. 0FGL J1830.3+0617

Source	RA (J2000)	Decl. (J2000)	Positional error	Count rate (0.3–10 keV)	HR $\frac{H-S}{H+S}$	N_{H} (cm^{-2})	ObsID
Swift J1830.1+0619	18:30:05.8	06:19:12	6."0	$(5.3 \pm 0.8) \times 10^{-2} \text{ s}^{-1}$	0.2	2.4×10^{21}	00039228001

Table 13. 0FGL J2001.0+4352

Source	RA (J2000)	Decl. (J2000)	Positional error	Count rate (0.3–10 keV)	HR $\frac{H-S}{H+S}$	N_{H} (cm^{-2})	ObsID
Swift J2001.1+4348	20:01:03.6	43:48:29	5."8	$(1.8 \pm 0.3) \times 10^{-3} \text{ s}^{-1}$	-0.08	3.7×10^{21}	00039229001
Swift J2001.2+4352	20:01:12.7	43:52:49	3."7	$(4.8 \pm 0.3) \times 10^{-2} \text{ s}^{-1}$	-0.54	3.7×10^{21}	00039229001

Table 14. 0FGL J2055.5+2540

Source	RA (J2000)	Decl. (J2000)	Positional error	Count rate (0.3–10 keV)	HR $\frac{H-S}{H+S}$	N_{H} (cm^{-2})	ObsID
Swift J2055.8+2546	20:55:48.5	25:46:35	5."4	$(4.0 \pm 1.0) \times 10^{-3} \text{ s}^{-1}$	-0.05	1.1×10^{21}	00031391001
Swift J2055.8+2540	20:55:50.3	25:40:49	6."0	$(3.2 \pm 1.1) \times 10^{-3} \text{ s}^{-1}$	0.07	1.1×10^{21}	00031391001

Table 15. 0FGL J2241.7–5239

Source	RA (J2000)	Decl. (J2000)	Positional error	Count rate (0.3–10 keV)	HR $\frac{H-S}{H+S}$	N_{H} (cm^{-2})	ObsID
Swift J2241.5–5246	22:41:33.3	-52:46:34	5.''4	$(5.4 \pm 1.3) \times 10^{-3} \text{ s}^{-1}$	-0.33	1.2×10^{20}	00031384001

Table 16. 0FGL J2302.9+4443

Source	RA (J2000)	Decl. (J2000)	Positional error	Count rate (0.3–10 keV)	HR $\frac{H-S}{H+S}$	N_{H} (cm^{-2})	ObsID
Swift J2302.1+4445	23:02:08.7	44:45:33	6.''7	$(2.3 \pm 0.8) \times 10^{-3} \text{ s}^{-1}$	-0.83	1.3×10^{21}	00031346001
	23:02:08.7	44:45:33	–	$< 8.0 \times 10^{-4} \text{ s}^{-1}$	–	1.3×10^{21}	00031346002

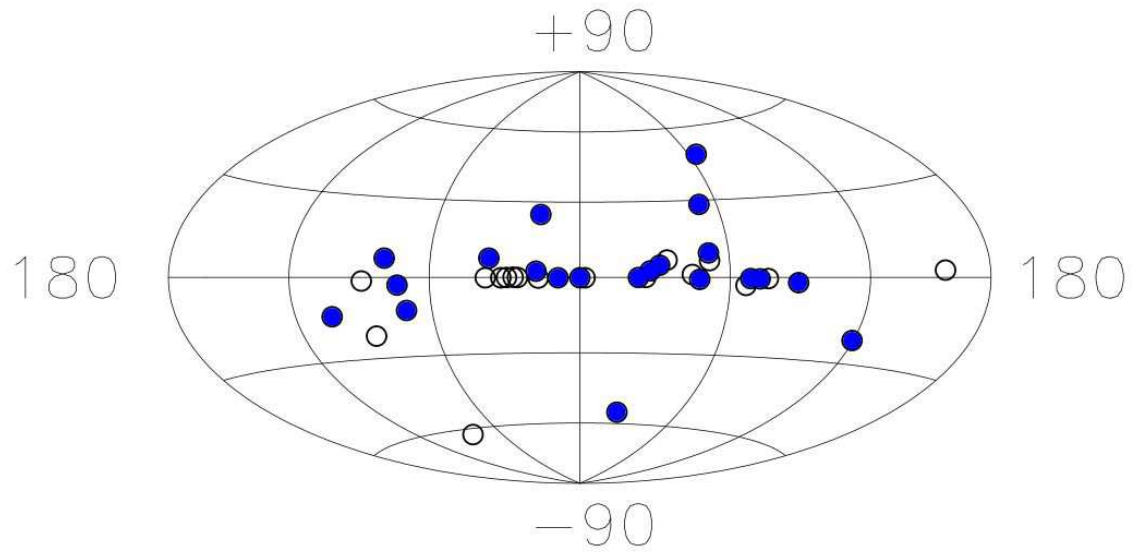


Fig. 1.—: Locations of unidentified 0FGL sources listed in Abdo et al. (2009b). Shaded symbols indicate sources observed by *Swift*.